IEEE Access
Multidisciplinary | Rapid Review | Open Access Journal

Received June 22, 2017, accepted July 13, 2017, date of current version August 22, 2017.

Digital Object Identifier 10.1109/ACCESS.2017.2731398

Phased Array Radar-Based Channel Modeling and Sparse Channel Estimation for an Integrated Radar and Communication System

LING HUANG[1,2,3], YU ZHANG[1,2,3,4], (Senior Member, IEEE), QINGYU LI[1,2,3], AND JIAN SONG[1,2,4], (Fellow, IEEE)

[1]Tsinghua National Laboratory for Information Science and Technology, Tsinghua University, Beijing 100084, China
[2]Department of Electronics Engineering, Tsinghua University, Beijing 100084, China
[3]Science and Technology on Information Transmission and Dissemination in Communication Networks Laboratory, Shijiazhuang 050081, China
[4]Shenzhen City Key Laboratory of Digital TV System, Shenzhen 518057, China

Corresponding author: Ling Huang (huangling13@mails.tsinghua.edu.cn)

This work was supported in part by the Science, Technology and Innovation Commission of Shenzhen Municipality under Grant JCYJ20150402103811550 and in part by the Science and Technology on Information Transmission and Dissemination in Communication Networks Laboratory under Grant KX132600028 and Grant ITDU15005/KX152600014.

ABSTRACT An integrated radar and communication system can cooperatively form a radar-communication network with significantly enhanced efficiency and considerably less occupied hardware resources. Such a system exhibits great advantages compared with traditional individual radar and communication modes. Numerous papers have proposed achieving the integrated functions based on phased array radar, whereas the channel modeling and channel estimation problems concerning communications are seldom discussed in the literature. In this paper, we propose a ray-cluster-based spatial channel model and a sounding channel estimation scheme realized on the existing hardware of phased array radar. Considering the correlation, we model the channel by comparing the difference between adjacent antennas, and we present the response vector of the antenna array. We analyze the number of beams that are needed to cover the space, and we present the sequence of directional beamforming vectors when sounding the channel. Redundant dictionary matrices are utilized to present the channel as a sparse signal recovery problem, in which the spatial sparsity is leveraged for performance enhancement. A sparsity adaptive matching pursuit (SAMP)-based compressed sensing tool is exploited for the sparse recovery problem and compared with the conventional least squares (LS) algorithm. The experimental results demonstrate that our proposed scheme can effectively solve the channel estimation problem in the integrated radar and communication system with reduced complexity, and it outperforms LS by 25% when considering mean square error (MSE) performance in general.

INDEX TERMS Integrated radar and communication systems, channel model, channel estimation, beamforming pattern, sparsity, sparsity adaptive matching pursuit.

I. INTRODUCTION

Wireless communication and radar sensing are two of the most important applications of radio technology, and these applications have previously been designed and developed in different manners. However, due to the high similarity of transceiver structures, the integration of these two applications is feasible, which means that they can somehow be combined to share hardware resources, and related processing work is needed in signal generation and separation [1]–[3]. There is no doubt that a successfully integrated system could provide many advantages, such as structure simplification, cost reduction and interference mitigation [4]. Furthermore, transceivers that perform both radar and communication functions can cooperatively form a radar-communication network, which will significantly enhance the work efficiency of the entire system [5], [6]. Accordingly, the integration of radar and communication with multi-functional capabilities can dramatically enhance the system efficiency, and it has attracted substantial attention from academic researchers.

Over the past several decades, the Office of Naval Research has been engaged in this field, and they launched a program called the Advanced Multifunction Radio Frequency Concept (AMRFC) in 1996, which aimed to share a common broadband antenna array to achieve multi-task capabilities

of radar and communication [7]. However, the preceding program only presented a conceptual introduction to the integrated system and did not investigate the technical issues concerning communication. Recently, numerous works have proposed realizing communication functions by sharing the existing radar hardware, particularly the widely used phased array radar [8], [9]. Phased array radar enjoys a large antenna aperture, which can emit signals with power gain and strong directivity. However, in phased array radar-based integrated radar-communication systems, reasonable channel modeling and accurate channel estimation are essential for guaranteeing the system performance, although few studies have addressed these issues in detail. Reference [10] proposed a burst single-carrier frequency-domain equalization scheme for data transmission, but its channel model was still based on the traditional independently distributed Rayleigh fading channel, which was not in accordance with practical scenarios. Reference [11] used antennas of phased array radar to transmit signals, but they ignored the effect of beamforming processing in array radar mode. Our previous work [2] realized the channel estimation processing based on radar mode, but did not illustrate the channel model we chose. Therefore, in a phased array radar-based integrated radar and communication system, which type of channel model is suitable and how the compulsory channel estimation scheme is performed are worth investigating.

With respect to the channel model and the channel estimation scheme based on radar hardware, there are three main issues. First, in phased array radar, the antenna spacing is half the length of the carrier wave, which results in a correlation between array antennas in general [12]. This means that directly adopting the Rayleigh or Rice fading model is no longer accurate; therefore, the channel model should take the correlation between antennas into consideration. Second, there is only a single radio frequency (RF) chain in phased array radar (a sub-array structure where each RF chain is connected with each sub-array is not included); therefore, only one signal can be radiated at one time regardless of how many antennas are equipped in the radar array. Moreover, the phase shifters located with each antenna control the signal direction by forming a narrow beam in a specific direction [12], [13]. In radar mode, we can only transmit one signal at one time and in one direction, which indicates that the channel estimation scheme should be conducted by time and by direction successively. Third, integrated radar and communication systems are typically used in the open air regardless of airborne, shipboard or ground applications, where limited scatterers and reflectors are located within transmission space [14]. Consequently, the channel presents spatial sparsity characteristics, which can be leveraged for improving performance and simplifying calculations. Accordingly, in phased array radar-based integrated radar and communication systems, the above three issues should be taken into account for the channel model and channel estimation scheme.

In the remainder of this paper, based on phased array radar, we consider a ray-cluster-based spatial channel model and propose a sounding channel estimation scheme for the integrated radar and communication systems. First, considering the correlation between antennas, we model the difference in the response between adjacent antennas and provide the steering vector of an essentially located antenna array. The channel is modeled by physical multipaths between the transmitter and receiver, each with an attenuation and AOA (angle of arrival)/AOD (angle of departure). Second, due to the limited resolvability in the angular domain of the antenna array, we analyze the number of beams required to cover the space when sounding the channel. The above two points are not fully explained in the previous work [2]. Third, considering that the channel sounding is conducted by direction and by time successively, we provide a sequence of beamforming vectors to probe the channel, and the corresponding outputs are collected as the observations. Fourth, we leverage the compressive sensing-based redundant dictionary matrix to present the channel as a sparse signal recovery problem, and we solve it using the same sparsity adaptive matching pursuit (SAMP)-based algorithm in [2]. The experimental results show that our proposed method can solve the channel estimation problem effectively with reduced complexity, and it outperforms the LS algorithm by 25% in general.

The remainder of this paper is organized as follows. Section II presents the ray-cluster channel model that is suitable for integrated radar and communication systems. The resolvability in the angular domain, beamforming processing and channel sounding-based scheme are presented in Section III. The compressed sensing-based redundant dictionary channel transformation and SAMP-based channel estimation algorithm are formulated in Section IV. The experimental results of the proposed algorithm compared with the traditional LS algorithm are presented in Section V. Finally, the conclusions are drawn in Section VI.

Notations: Bold uppercase $\mathbf{A}$ is used to denote matrices while lowercase $\mathbf{a}$ is used to denote a vector. Superscripts $\mathbf{A}^*$, $\mathbf{A}^T$, $\mathbf{A}^H$, $\mathbf{A}^{-1}$, $\mathbf{A}^\dagger$ are used to denote the conjugate, transport, the conjugate transport, the inverse and the pseudo-inverse of the matrix $\mathbf{A}$, resp. $\|\boldsymbol{A}\|_F$ is the Frobenius norm. $\mathbf{I}_N$ denotes the $N \times N$ identity matrix and $\mathbb{E}(\mathbf{A})$ means the expectation operator. Moreover, $c \sim \mathcal{CN}(\mu, \sigma^2)$ indicates c is complex Gaussian distributed with mean μ and variance σ^2.

II. CHANNEL MODELING OF INTEGRATED RADAR AND COMMUNICATION SYSTEMS

In this section, we would like to obtain some insights regarding the phased array radar-based wireless channel model. A narrowband channel representation is considered in the following.

A. UNIFORM LINEAR ANTENNA ARRAY's RESPONSE VECTOR OF FAR-FIELD SIGNAL

Consider a far-field signal received directly by an antenna array as shown in Figure 1.(a), where 'Tx' and 'Rx' denote 'transmit' and 'receive', respectively. A uniform linear antenna (ULA) array is considered, in which the antennas

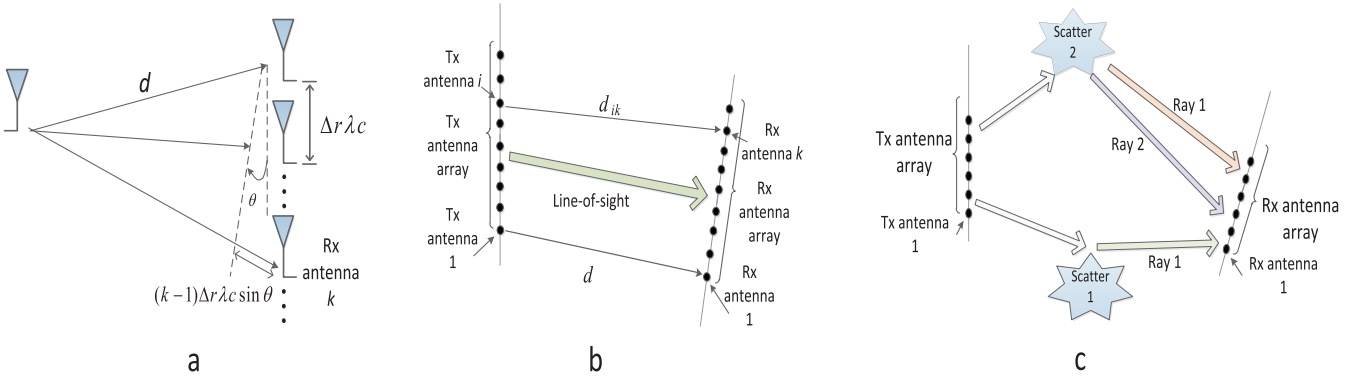

FIGURE 1. Illustration of wireless channel model based on antenna array: (a) a far-field signal received directly by an antenna array; (b) line-of-sight channel model of uniform linear antenna array; (c) ray-cluster-based spatial channel model of uniform linear antenna array.

are evenly spaced on a straight line. The number of receive antennas is N. Let $\Delta\lambda_c$ denotes the antenna spacing, where λ_c is the carrier wavelength and Δ is the normalized antenna spacing, which is normalized to the carrier wavelength. In a phased array radar system, Δ is primarily set as $\frac{1}{2}$. Note that the dimension of the antenna array is supposed to be considerably smaller than the distance between the signal generator and the receiver. The impulse response $h_k(\tau)$ from the transmitter to the kth receive antenna is

$$h_k(\tau) = \beta\delta(\tau - d_k/c), \quad k = 1, \ldots, N, \tag{1}$$

where c is the speed of light, d_k is the distance between the signal generator and the kth receive antenna, and β is the attenuation of the transmission path, which is supposed to be the same for all the receive antennas. Suppose that $d_k/c \ll 1/W$, where W is the signal bandwidth. According to [15], the channel gain can be written in another form as

$$h_k = \beta exp(-\frac{j2\pi f_c d_k}{c}) = \beta exp(-\frac{j2\pi d_k}{\lambda_c}), \tag{2}$$

where f_c is the carrier frequency. Since the distance between the signal generator and the receiver is much larger than the size of the antenna array, the paths to each of the receive antennas are approximately equal to its first order:

$$d_k \approx d + (k-1)\Delta\lambda_c \sin\theta, \quad k = 1, \ldots, N, \tag{3}$$

where d is the distance from the signal generator to the first (or nearest) receive antenna and θ is the incident angle to the receive antenna array. Accordingly, the vector of channel gains $\mathbf{h} = [h_1, h_2, \ldots, h_N]^T$ can be written as

$$\mathbf{h} = \beta exp(-\frac{j2\pi d}{\lambda_c}) \begin{bmatrix} 1 \\ e^{-j2\pi\Delta\sin\theta} \\ e^{-j2\pi 2\Delta\sin\theta} \\ \vdots \\ e^{-j2\pi(N-1)\Delta\sin\theta} \end{bmatrix}, \tag{4}$$

which indicates that the channel responses of serial receive antennas vary in phase by $2\pi\Delta\sin\theta$ due to the time delay. Here, we define a response vector of the channel as

$$\mathbf{a}(\theta) = \frac{1}{\sqrt{N}} \begin{bmatrix} 1 \\ e^{-j2\pi\Delta\sin\theta} \\ e^{-j2\pi 2\Delta\sin\theta} \\ \vdots \\ e^{-j2\pi(N-1)\Delta\sin\theta} \end{bmatrix}. \tag{5}$$

In fact, the channel response of the transmit antennas is reciprocal to that of the receive antennas, just replacing the corresponding departure angle and the number of antennas.

B. LINE-OF-SIGHT CHANNEL MODEL OF UNIFORM LINEAR ARRAY

Now consider the wireless channel with uniform linear array antennas on both sides. Suppose that there is only one direct line-of-sight path between the antennas, as shown in Fig. 1.(b). The normalized antenna spacings are Δ_t and Δ_r of the transmitter and the receiver, respectively, and are set to be $\frac{1}{2}$ in phased array radar. The channel gain between the ith transmit antenna and the kth receive antenna is

$$h_{ik} = \beta exp(-j2\pi d_{ik}/\lambda_c), \tag{6}$$

where d_{ik} is the distance between the corresponding antennas and β is the path attenuation, which is assumed to be identical for all antenna pairs. Similar to (3), the distance d_{ik} can be approximated to its first order as follows:

$$d_{ik} = d + (k-1)\Delta_r\lambda_c \sin\theta_r - (i-1)\Delta_t\lambda_c \sin\theta_t, \tag{7}$$

where d is the distance between transmit antenna 1 and receive antenna 1 (also the nearest pair) and θ_t and θ_r are the angles of arrival and departure of the path on the transmit and receive antenna arrays, respectively. By replacing (6) with (7), the channel gain can be rewritten as

$$h_{ik} = \beta exp(-\frac{j2\pi d}{\lambda_c}) \cdot exp(j2\pi(i-1)\Delta_t \sin\theta_t) \cdot exp(-j2\pi(k-1)\Delta_r \sin\theta_r). \tag{8}$$

Accordingly, the channel matrix of the uniform linear antenna array on both sides can be written as

$$\mathbf{H} = \beta\sqrt{N_t N_r}exp(-\frac{j2\pi d}{\lambda_c})\mathbf{a}_r(\theta_r)\mathbf{a}_t(\theta_t)^H, \tag{9}$$

where N_t and N_r are the numbers of antennas of the transmitter and receiver, respectively, and $\mathbf{a}_r(\theta_r)$ and $\mathbf{a}_t(\theta_t)$ are defined in (5).

C. RAY-CLUSTER-BASED SPATIAL CHANNEL MODEL

Now suppose that there is an arbitrary number of physical paths that may pass through the scatterers and reflectors between the transmitter and the receiver. With the lth path having an attenuation of β_l, an angle θ_t^l of the transmit antenna and an angle θ_r^l of the receive antenna array, the channel matrix $\mathbf{H}$ of the uniform linear antenna array is written as

$$\mathbf{H} = \sqrt{N_t N_r}\sum_{l=1}^{N_p}\alpha_l\mathbf{a}_r(\theta_r^l)\mathbf{a}_t(\theta_t^l)^H, \tag{10}$$

where

$$\alpha_l = \beta_l exp(-\frac{j2\pi d^l}{\lambda_c}), \tag{11}$$

$$\mathbf{a}_t(\theta_t) = \frac{1}{\sqrt{N_t}}\begin{bmatrix} 1 \\ e^{-j2\pi\Delta_t\sin\theta_t} \\ e^{-j2\pi 2\Delta_t\sin\theta_t} \\ \vdots \\ e^{-j2\pi(N_t-1)\Delta_t\sin\theta_t}\end{bmatrix}, \tag{12}$$

$$\mathbf{a}_r(\theta_r) = \frac{1}{\sqrt{N_r}}\begin{bmatrix} 1 \\ e^{-j2\pi\Delta_r\sin\theta_r} \\ e^{-j2\pi 2\Delta_r\sin\theta_r} \\ \vdots \\ e^{-j2\pi(N_r-1)\Delta_r\sin\theta_r}\end{bmatrix}, \tag{13}$$

additionally, N_p is the total number of paths, and d^l is the distance between transmit antenna 1 and receive antenna 1 (or the nearest pair) along path l. $\mathbf{a}_t(\theta)$ and $\mathbf{a}_r(\theta)$ are the response vectors of the transmit and receive antenna arrays, respectively.

In fact, one incident signal passing through one scatterer may generate more than one outgoing signal in different directions, and a more accurate channel model is based on a ray cluster [16], where N_c denotes the number of clusters and N_r denotes the number of rays in one specific cluster. We illustrate this model in Fig. 3.(c). The channel can be written as

$$\mathbf{H} = \sqrt{N_t N_r}\sum_{c=1}^{N_c}\sum_{r=1}^{N_r}\alpha_{c,r}\mathbf{a}_r(\theta_r^{c,r})\mathbf{a}_t(\theta_t^{c,r})^H, \tag{14}$$

where $\alpha_{c,r}$, $\theta_t^{c,r}$ and $\theta_r^{c,r}$ denote the complex gain, AOA and AOD of ray r in cluster c, respectively, and $\mathbf{a}_t$ and $\mathbf{a}_r$ denote the array response vectors for the transmit and receive antenna arrays, respectively.

The channel model that we discussed above is restricted to uniform linear antenna arrays; for other geometrical structures of antenna arrays, the major difference is that the response vectors vary due to the different delay responses of the antennas. By simply replacing the antenna response vectors, one can obtain the channel models of other array structures (more details are explained in [17]). More importantly, the scheme and estimation that we subsequently present are applicable to any array structure.

III. PHASED ARRAY RADAR-BASED CHANNEL SOUNDING SCHEME

In this section, we still adopt a uniform linear antenna array as an example. First, the numbers of transmit and receive beams that are needed are illustrated in terms of the resolvability of the antenna array in the angular domain. Then, we present the beamforming processing in radar mode. Finally, the channel sounding scheme based on phased array radar is described.

A. RESOLVABILITY OF THE ANTENNA ARRAY IN THE ANGULAR DOMAIN

In this section, we illustrate the resolvability of the antenna array in the angular domain. Only consider the two-dimensional plane. Let $L_t := N_t\Delta_t$ and $L_r := N_r\Delta_r$ denote the normalized lengths of the transmit and receive antenna arrays, respectively. The paths arrive from different directions, and the parameter $1/L_r$ ($1/L_t$ is the same) can be viewed as a measure of resolvability from the perspective of the angular domain [17]. Similar to the role that the bandwidth W plays in the wireless channel, the parameter $1/W$ measures the resolvability of the signals in the time domain, and multipaths that arrive at time intervals that are much less than $1/W$ cannot be distinguished by the receiver; signals that arrive within an angle that is much less than $1/L_r$ cannot be distinguished by the receive antenna either ([15] is recommended for further explanation). Specifically, take the receiver as an example, and let θ_{r1} and θ_{r2} denote two different arrival directions; if

$$|\theta_{r1} - \theta_{r2}| < 1/L_r, \tag{15}$$

then the paths of these two directions cannot be distinguished by the receive antenna array, and they are aggregated to be viewed as one path.

All of the above suggest that we should 'sample' the channel in the space angular domain at a fixed angular interval of $1/L_t$ at the transmitter and at a fixed angular interval of $1/L_r$ at the receiver. Let the angle θ vary from $[-\frac{\pi}{2}, \frac{\pi}{2}]$; accordingly, the angular value $sin\theta$ ranges from -1 to 1, and the entire angular scope is 2. Therefore, the numbers of resolvable bins are as follows:

$$\frac{2}{1/L_t} = 2L_t = 2N_t\Delta_t = N_t, \tag{16}$$

$$\frac{2}{1/L_r} = 2L_r = 2N_r\Delta_r = N_r, \tag{17}$$

where Δ_t and Δ_r are normalized antenna spacings and are set to be $\frac{1}{2}$. Accordingly, to sound the channel and cover the space

completely, every resolvable bin should transmit or receive a beam. This means that the number of transmit beams should equal the number of resolvable bins at the transmitter and the number of receive beams should equal the number of resolvable bins at the receiver. The mathematical formulation of the above conclusion is as follows:

$$M_t = \frac{2}{1/L_t} = N_t, \tag{18}$$

$$M_r = \frac{2}{1/L_r} = N_r, \tag{19}$$

where M_t and M_r denote the numbers of beams to be transmitted and received, respectively.

B. BEAMFORMING PROCESSING OF PHASED ARRAY RADAR

Radars perform beamforming to achieve long-range detection and tracking. Communication operations should follow the typical radar mode since the integration of radar and communication is based on existing radar hardware. Specifically, there are some basic principles of phased array radar as follows. First, through beamforming processing, the radiated signals from individual antennas are coherently stacked to form a beam in a given direction. Then, by adjusting the value of the phase shifter located with every antenna, phased array radar can generate the directional narrow beams that it needs. Moreover, because only a single RF chain is connected to an antenna array (a sub-array structure where each RF chain is connected to a specific sub-array is not included), even though there are a multitude of antennas in the array, all the antennas can only transmit the same signal (could still have different phase shifts) at one time. All of the above indicate that based on radar hardware, the communication operation is conducted by time and by direction sequentially.

Consider the ULA antenna array at the transceivers; the beamforming processing of radar is shown in Fig. 2. The radiation function of ϕ-angle from the array boresight is

$$|F(\phi)| = \frac{\sin N\pi\Delta(\sin\phi - \sin\phi_b)}{\sin\pi\Delta(\sin\phi - \sin\phi_b)}, \tag{20}$$

where ϕ is the target orientation, ϕ_b is the beam transmitting direction of the array, N is the number of antennas, and Δ is the normalized antenna spacing, which equals $\frac{1}{2}$ [12]. From (20), we observe that when $\phi_b = \phi$, the radiation function obtains the maximum. In other words, to form a ϕ-direction beam, the antenna array beamforming vector $\mathbf{b}(\phi) \in^{N\times 1}$ is as shown below:

$$\mathbf{b}(\phi) = \frac{1}{\sqrt{N}}[1\ e^{-j\varphi}\ \ldots\ e^{-j(N-1)\varphi}]^T, \tag{21}$$

where $\varphi = 2\pi\Delta\sin\phi$ is the corresponding phase shift from element to element along the antenna array.

Let M denote the number of generated beam patterns, and consider that the entire radiation direction varies from $-\frac{\pi}{2}$ to $\frac{\pi}{2}$ of a two-dimensional plane; therefore, each beam's target orientation is from a finite set $\phi_m \in \{-\frac{\pi}{2}, -\frac{\pi}{2}+\frac{\pi}{M}, -\frac{\pi}{2}+\frac{m\pi}{M}, \ldots, \frac{\pi}{2}-\frac{\pi}{M}\}, m = 0, 1, \ldots, M-1$.

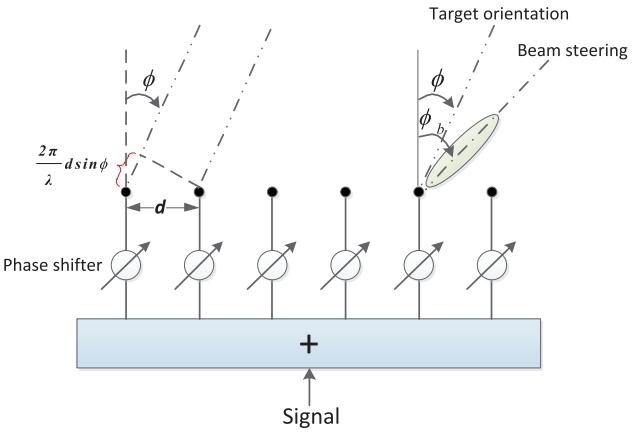

FIGURE 2. Beamforming processing in phased array radar.

C. BEAM SOUNDING SCHEME FOR CHANNEL ESTIMATION

Consider a point-to-point communication situation based on the phased array radar shown in Fig. 3, where the transmitter and the receiver are equipped with N_t and N_r antennas, respectively. During the beam sounding period for channel estimation, the transmitter and the receiver successively radiate and receive the non-overlapped directional beams. Since both the transmitter and the receiver have only a single RF chain, they can generate only one sounding beam at one time. We assume that the channel changes slowly, and the transceiver could exploit the channel reciprocity. To sound the space of the channel, the transmitter adopts M_t beamforming patterns denoted as $\{\mathbf{b}_t^{m_t} = \mathbf{b}(\phi_{m_t}), m_t = 0, 1, \ldots, M_t - 1, \phi_{m_t} = -\frac{\pi}{2} + \frac{\pi\cdot m_t}{M_t}\}$, and the receiver adopts M_r beamforming patterns denoted as $\{\mathbf{b}_r^{m_r} = \mathbf{b}(\phi_{m_r}), m_r = 0, 1, \ldots, M_r - 1, \phi_{m_r} = -\frac{\pi}{2} + \frac{\pi\cdot m_r}{M_r}\}$, where $\mathbf{b}(\phi)$ is defined in (21). Since there are N_t and N_r resolvable bins in the angular domain at the transmitter and the receiver, respectively, the number of sounding beams should equal the number of antennas, which is the conclusion that we reached in the previous section.

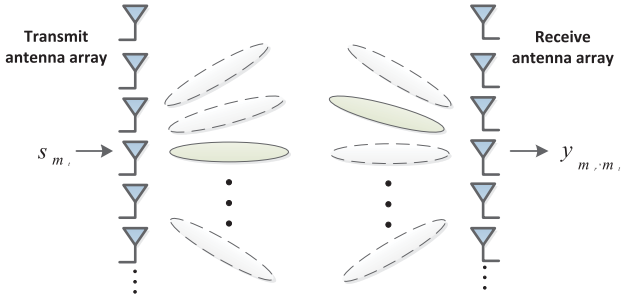

FIGURE 3. Channel sounding processing of the integrated system.

During the sounding phase, the transmitter sequentially radiates $\{\mathbf{b}_t^{m_t}\}$ sounding beams, and each beam is received by the receiver through its beam patterns $\{\mathbf{b}_r^{m_r}\}$, as shown in the figure. The output observation for the m_rth received beam and

the m_tth transmitted beam is given below:

$$y_{m_r,m_t} = \sqrt{\gamma}(\mathbf{b}_r^{m_r})^H \mathbf{H}\mathbf{b}_t^{m_t} s_{m_t} + (\mathbf{b}_r^{m_r})^H n_{m_r,m_t}, \quad (22)$$

where γ is the transmit power, $\mathbf{H} \in \mathbb{C}^{N_r \times N_t}$ is the channel matrix that is to be estimated, s_{m_t} is the transmitted pilot associated with the beamforming pattern $\mathbf{b}_t^{m_t}$, and n_{m_r,m_t} is the interference noise with respect to $\mathcal{CN}(0, \sigma^2)$. Collecting y_{m_r,m_t} for $m_r \in \{1, \ldots, M_r\}$ and $m_t \in \{1, \ldots, M_t\}$, we obtain

$$\mathbf{Y} = \sqrt{\gamma}\mathbf{B}_r^H \mathbf{H}\mathbf{B}_t\mathbf{S} + \mathbf{B}_r^H\mathbf{N}, \quad (23)$$

where $\mathbf{Y} \in \mathbb{C}^{M_r \times M_t}$, $\mathbf{B}_r = \{\mathbf{b}_r^0, \ldots, \mathbf{b}_r^{M_r-1}\} \in \mathbb{C}^{N_r \times M_r}$, $\mathbf{B}_t = \{\mathbf{b}_t^0, \ldots, \mathbf{b}_t^{M_t-1}\} \in \mathbb{C}^{N_t \times M_t}$, and $\mathbf{N} \in \mathbb{C}^{M_r \times M_t}$. $\mathbf{S}$ is a diagonal matrix with M_t transmitted pilots s_{m_t}, where $m_t = 1, \ldots, M_t$ on its diagonal. Due to the distinction in the direction of the sounding beams, the transmitted pilots can be equal, i.e., $\mathbf{S} = \mathbf{I}_{M_t}$, and therefore, (23) can be written as

$$\mathbf{Y} = \sqrt{\gamma}\mathbf{B}_r^H \mathbf{H}\mathbf{B}_t + \mathbf{B}_r^H\mathbf{N}. \quad (24)$$

By sounding the space in beams, we have collected the channel information that we need up to now. The next step is to estimate the channel values that we obtained.

IV. SPARSE CHANNEL REPRESENTATION AND SAMP-BASED CHANNEL ESTIMATION ALGORITHM

In this section, we first use the dictionary matrix to transform the channel into a sparse one. Then, we adopt the SAMP-based algorithm to estimate the channel. Finally, the computational complexity of SAMP compared with LS is analyzed.

A. SPARSITY REPRESENTATION OF THE CHANNEL

Although the channel form in (14) is the practical physical model, it can be written in a more compact way as follows:

$$\mathbf{H} = \mathbf{A}_r\mathbf{H}_a\mathbf{A}_t^H, \quad (25)$$

where $\mathbf{H}_a = \sqrt{N_t N_r}diag(\alpha_1, \ldots, \alpha_{N_p})$, $\mathbf{A}_t = [\mathbf{a}_t(\theta_t^1), \ldots, \mathbf{a}_t(\theta_t^{N_p})] \in^{N_t \times N_p}$, and $\mathbf{A}_r = [\mathbf{a}_r(\theta_r^1), \ldots, \mathbf{a}_r(\theta_r^{N_p})] \in^{N_r \times N_p}$, $N_p = N_c \times N_r$.

Considering the transmission environment where limited scatterers are located, the channel model in the integrated radar-communication system is low rank, which is explicitly reflected in the sparse nature of the channel matrix $\mathbf{H}$. Next, we need to use the general redundant dictionary matrices to represent the channel in its sparse way.

Now let AOAs/AODs be taken from a uniform grid of angle in terms of size G, i.e., $\theta_t^{c,r}, \theta_r^{c,r} \in \{-\frac{\pi}{2}, -\frac{\pi}{2} + \frac{\pi}{G}, \ldots, \frac{\pi}{2} - \frac{\pi}{G}\}$, with $G \gg N_p$ to achieve the desired resolution. Define the array response matrices whose columns are the array response vectors corresponding to the candidate angles in the grid, as $\overline{\mathbf{A}}_t, \overline{\mathbf{A}}_r$. Specifically, $\overline{\mathbf{A}}_t = [\mathbf{a}_t(-\frac{\pi}{2}), \mathbf{a}_t(-\frac{\pi}{2} + \frac{\pi}{G}) \ldots, \mathbf{a}_t(\frac{\pi}{2} - \frac{\pi}{G})] \in \mathbb{C}^{N_t \times G}$, and $\overline{\mathbf{A}}_r = [\mathbf{a}_r(-\frac{\pi}{2}), \mathbf{a}_r(-\frac{\pi}{2} + \frac{\pi}{G}) \ldots, \mathbf{a}_r(\frac{\pi}{2} - \frac{\pi}{G})] \in \mathbb{C}^{N_r \times G}$. Using these grid matrices, the channel matrix $\mathbf{H}$ in (25) can be approximated with an N_p-sparse matrix $\mathbf{H}_b \in \mathbb{C}^{G \times G}$, i.e., $\mathbf{H} \approx \overline{\mathbf{A}}_r\mathbf{H}_b\overline{\mathbf{A}}_t^H$. Note that while $\mathbf{H}_a \in \mathbb{C}^{N_p \times N_p}$ is diagonal, $\mathbf{H}_b$ is not a diagonal but a sparse matrix. There is grid error in the above approximation since the actual AOAs/AODs do not necessarily fall into the uniform grid of the angles. Moreover, this error could be mitigated or even neglected along with the increase in the number of the grid G. Ignoring the error, the channel matrix can be written as follows:

$$\mathbf{H} = \overline{\mathbf{A}}_r\mathbf{H}_b\overline{\mathbf{A}}_t^H. \quad (26)$$

Here, we obtain the sparse representation of the channel. $\overline{\mathbf{A}}_t$ and $\overline{\mathbf{A}}_r$ are also called dictionary matrices (also a type of transform base) in compressed sensing theory [18], which could transform the matrix into its sparse counterpart. Since $\overline{\mathbf{A}}_t$ and $\overline{\mathbf{A}}_r$ are determined in advance, the unknown variable is only $\mathbf{H}_b$ when estimating $\mathbf{H}$.

B. SAMP-BASED SPARSE CHANNEL ESTIMATION ALGORITHM

Here, we obtain the observation result $\mathbf{Y}$ of channel H and the dictionary matrices $\overline{\mathbf{A}}_t$ and $\overline{\mathbf{A}}_r$; the next step is to estimate the sparse $\mathbf{H}_b$. To address this estimation problem, we first vectorize the matrix $\mathbf{Y}$. Using $\overline{\mathbf{y}}$ to denote the vec($\mathbf{Y}$), (24) is rewritten as

$$\overline{\mathbf{y}} = \sqrt{\gamma}(\mathbf{B}_t^T \otimes \mathbf{B}_r^H) \cdot vec(\mathbf{H}) + \overline{\mathbf{n}} = \mathbf{P} \cdot vec(\mathbf{H}) + \overline{\mathbf{n}}, \quad (27)$$

where this equality comes from the identity $vec(\mathbf{ABC}) = (\mathbf{C}^T \otimes \mathbf{A}) \cdot vec(\mathbf{B})$, $\overline{\mathbf{n}} = vec(\mathbf{N})$, and $\mathbf{P} = \sqrt{\gamma}\mathbf{B}_t^T \otimes \mathbf{B}_r^H \in \mathbb{C}^{M_tM_r \times N_tN_r}$. Given (27), a common approach to compute vec($\mathbf{H}$) is to use the conventional LS estimator, which solves the problem by computing $vec(\mathbf{H}) = (\mathbf{P}^H\mathbf{P})^{-1}\mathbf{P}^H\overline{\mathbf{y}}$ and only requires $M_tM_r \geq N_tN_r$. However, directly adopting the LS algorithm could lead to prohibitive computational operations, which is unacceptable in real systems. Hence, exploiting the spatial sparsity properties of the physical channel is quite essential. By transforming to the sparse channel form, we propose a compressed sensing-based channel estimation algorithm, which can significantly reduce the complexity while maintaining satisfactory performance.

Rewrite (27) in terms of the transformed sparse channel coefficients as

$$\begin{aligned}\overline{\mathbf{y}} &= \sqrt{\gamma}(\mathbf{B}_t^T \otimes \mathbf{B}_r^H) \cdot vec(\overline{\mathbf{A}}_r\mathbf{H}_b\overline{\mathbf{A}}_t^H) + \overline{\mathbf{n}} \\ &= \sqrt{\gamma}(\mathbf{B}_t^T \otimes \mathbf{B}_r^H) \cdot (\overline{\mathbf{A}}_t^* \otimes \overline{\mathbf{A}}_r) \cdot vec(\mathbf{H}_b) + \overline{\mathbf{n}} \\ &= \sqrt{\gamma}(\mathbf{B}_t^T \cdot \overline{\mathbf{A}}_t^*) \otimes (\mathbf{B}_r^H \cdot \overline{\mathbf{A}}_r) \cdot vec(\mathbf{H}_b) + \overline{\mathbf{n}} \\ &= \overline{\mathbf{P}} \cdot vec(\mathbf{H}_b) + \overline{\mathbf{n}}, \end{aligned} \quad (28)$$

where this equality follows from $(\mathbf{A} \otimes \mathbf{B}) \cdot (\mathbf{C} \otimes \mathbf{D}) = (\mathbf{A} \cdot \mathbf{C}) \otimes (\mathbf{B} \cdot \mathbf{D})$, and $\overline{\mathbf{P}} = \sqrt{\gamma}(\mathbf{B}_t^T \cdot \overline{\mathbf{A}}_t^*) \otimes (\mathbf{B}_r^H \cdot \overline{\mathbf{A}}_r) \in \mathbb{C}^{M_tM_r \times N_tN_r}$. Now, the N_p-sparse vector $vec(\mathbf{H}_b) \in \mathbb{C}^{G^2 \times 1}$ can be recovered using the sensing matrix $\overline{\mathbf{P}}$. CS tools can be leveraged to solve this problem. The compressed sensing theory-based optimization expression for the sparse channel estimation is as follows [19]:

$$\begin{aligned}&\min_{vec(\widehat{\mathbf{H}}_b)} \|vec(\widehat{\mathbf{H}}_b)\|_0, \\ &s.t.\ \overline{\mathbf{y}} = \overline{\mathbf{P}}^H \cdot vec(\widehat{\mathbf{H}}_b). \end{aligned} \quad (29)$$

Since realistic channel characteristics are unknown to the transceivers before estimation, we need to select an appropriate sparse recovery method. The classic SAMP algorithm can solve the sparse recovery problem because it reconstructs the signals without the need for prior information about the sparsity level [2], [20], [21]. The processing using the SAMP algorithm to recover the channel gains is shown below.

1: **Input**: Observation vector $\overline{\mathbf{y}}$, sensing matrix $\overline{\mathbf{P}}$ and termination condition ε.
2: **Parameter initialization:** i=1, k=1, t=1 and $\mathbf{r}_0 = \overline{\mathbf{y}}$. % i,k,t,**r** denote the iteration index, stage index,step size and residue, respectively.
3: $\widetilde{\Omega} = \Omega = \widetilde{\Gamma} = \Gamma = \emptyset$; $\Lambda = t$. % Ω, Γ are the supporting sets, Λ denotes the sparsity level of the current stage.
4: **repeat**
5: $\Gamma_i = argmax_{\widetilde{\Gamma}}\{\|\overline{\mathbf{P}}^H \mathbf{r}_{i-1}\|_2, |\widetilde{\Gamma}| = \Lambda\}$. % choose the t maximum value, record the corresponding row index in $\overline{\mathbf{P}}$, and form the set Γ.
6: $\Lambda_i = \Omega_{i-1} \cup \Gamma_i$. % make candidate elements.
7: $\Omega = argmax_{\widetilde{\Omega}}\{\|\overline{\mathbf{P}}^{\dagger}_{\Lambda_i} \cdot \overline{\mathbf{y}}\|_2, |\widetilde{\Omega}| = \Lambda\}$. % choose the t maximum value, record the corresponding row index in $\overline{\mathbf{P}}^{\dagger}_{\Lambda_i}$, and form the set Ω.
8: $\mathbf{r} = \overline{\mathbf{y}} - \overline{\mathbf{P}}_{\Omega}\overline{\mathbf{P}}^{\dagger}_{\Omega} \cdot \overline{\mathbf{y}}$. % compute the residue.
9: **if** $\|\mathbf{r}\|_2^2 < \varepsilon$, **then**
10: quit the iteration.
11: **else if** $\|\mathbf{r}\|_2^2 \geq \|\mathbf{r}_{i-1}\|_2^2$, **then**
12: k=k+1; $\Lambda = j \times t$. % update the estimation stage.
13: **else**
14: $\Omega_i = \Omega$; $\mathbf{r}_i = \mathbf{r}$; $i = i+1$. % continue the estimation at the current stage.
15: **end if**
16: **until** $\|\mathbf{r}\|_2^2 \leq \varepsilon$.
17: **return** $\widehat{\mathbf{H}}_b = vec^{-1}(\overline{\mathbf{P}}^{\dagger}_{\Omega} \cdot \overline{\mathbf{y}})$.
18: **Output**: Sparse channel representation in vector form $\widehat{\mathbf{H}}_b$.

Specifically, in each stage with a Λ-sparsity level, steps 5 and 7 choose the t maximum value, record the corresponding row indices, and form a new set; step 6 presents the candidate list; and step 8 $\sim$ 11 computes the corresponding residual, and if the termination threshold is met, the algorithm is stopped. Otherwise, it updates the parameters and starts a new stage of calculation in steps 12 $\sim$ 17. Once we obtain the estimated output $\widehat{\mathbf{H}}_b$ and we already know the dictionary matrices ($\overline{\mathbf{A}}_t$ and $\overline{\mathbf{A}}_r$) that transformed the channel, the corresponding result of the estimated channel, denoted as $\widehat{\mathbf{H}}$, is written as

$$\widehat{\mathbf{H}} = \overline{\mathbf{A}}_r \widehat{\mathbf{H}}_b \overline{\mathbf{A}}_t^H. \tag{30}$$

C. COMPLEXITY ANALYSIS

In this section, we compare the computational complexity of the SAMP and the LS. The computation load of LS algorithm mainly comes from calculating pseudo inverse of matrix $\mathbf{P} \in \mathbb{C}^{M_t M_r \times N_t N_r}$. Its complexity is $\mathcal{O}((N_t N_r)^2 M_t M_r)$. When we analyse the SAMP algorithm, we can see that there still contains pseudo inverse operations in step 8, but note that not all the elements in $\overline{\mathbf{P}}$ but just some selected rows are involved in this operation, which means the computational complexity in this step is negligible. Therefore, for the SAMP based method, the computational complexity in each iteration mainly depends on the multiplication of $\overline{\mathbf{P}}^H$ and $\mathbf{r}_{i-1}$ with $\mathcal{O}(G^2 M_t M_r)$ complexity. Still take the total number of iterations T into consideration, the computational complexity of SAMP is $\mathcal{O}(TG^2 M_t M_r)$.

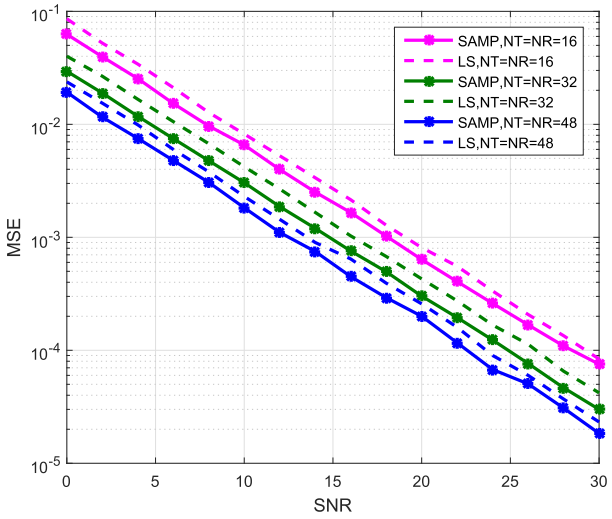

FIGURE 4. Mean square error (MSE) of channel estimation for the SAMP algorithm compared with the LS algorithm.

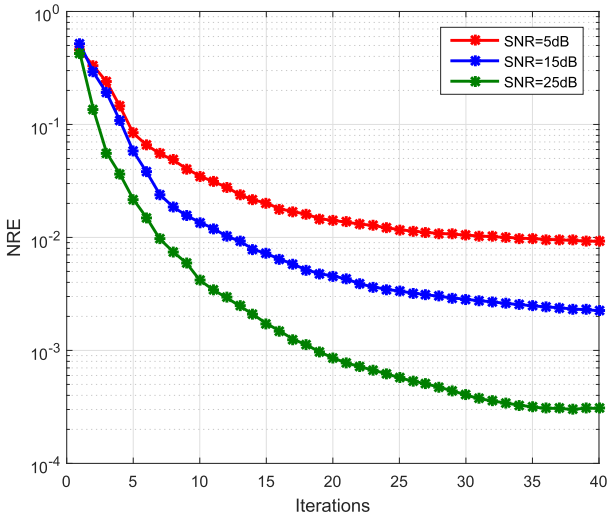

FIGURE 5. Convergence speed of the SAMP algorithm by computing the normalized residual error (NRE).

V. SIMULATION RESULTS

This section presents the simulation results of the proposed channel sounding scheme and the channel estimation algorithm of integrated radar and communication systems. The simulation parameters are set as follows. Both the transmitters and the receivers are equipped with uniform linear

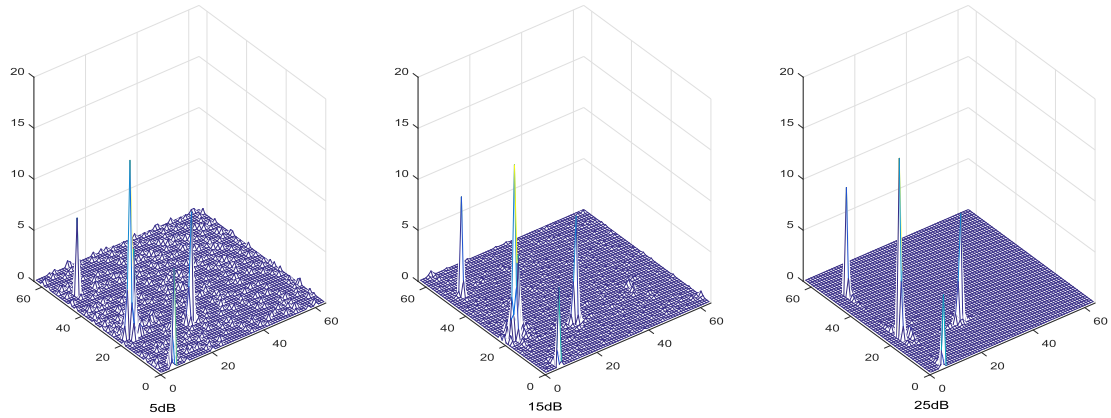

FIGURE 6. Distribution of the SAMP-based reconstructed distinct energy clusters of the sparse channel representation.

antennas. The numbers of antennas are set to be $N_t = N_r = 16, 32, 48$, and each side has only one RF chain. The grid size G is varied and compared according to different requirements. AOAs/AODs are randomly distributed between $[-\frac{\pi}{2}, \frac{\pi}{2}]$ in a two-dimensional plane. The transmit power γ is 1. The signal-to-noise ratio (SNR) is defined as $10\log 10(\gamma/\sigma^2)$. The number of transmitting and receiving beams is $M_t = N_t, M_r = N_r$. The conventional LS algorithm was also adopted for comparison.

In Fig. 4, we present the average mean square error (MSE) of channel estimation for both the SAMP algorithm and the LS algorithm, where the MSE is defined as $(\mathbb{E}[\|\widehat{\mathbf{H}} - \mathbf{H}\|_2^2/\|\mathbf{H}\|_2^2])$. The configurations in which both the transmitter and the receivers are equipped with $N_t = N_r = 16,\ 32\ and\ 48$ antennas are compared. The parameter of gird size G is 96. The channel model is set to be 4 clusters, each with 1 ray. As shown in Fig. 4, for all numbers of antennas, the MSE performances of SAMP are all better than those of LS, as expected, which is essentially because SAMP enjoys the sparse properties of the channel. Specifically, the proposed SAMP algorithm is 24.7% better than the LS estimator when SNR=16 dB. Moreover, the MSE decreases as the number of antennas increases. Take SNR=16 dB as an example; the MSE of 48 antennas is 39.6% better than that of 32 antennas, and it is 76.5% better than 16 antennas. This result is because more antennas can provide higher accuracy of spatial resolution and bring better estimation results.

In Fig. 5, we present the convergence speed of the SAMP algorithm by computing the normalized residual error (NRE) at the ith iteration, which is defined as $NRE_i = \|\mathbf{r}_i\|_2^2/\|\bar{\mathbf{y}}\|_2^2$. The number of antennas on both sides is set to be $N_t = N_r = 32$ with grid size G=64, and the observation result NRE is evaluated at SNR=5 dB, 15 dB and 25 dB. The channel model is set to be 4 clusters, each with 1 ray. As shown in Fig. 5, the algorithm outputs a sufficiently small residual after 20∼30 iterations and reaches a steady state, which means that the total number of iterations T approximately equals this order of magnitude. Specifically, for $N_t = N_r = 32$ and $G = 64$, the computational complexity of SAMP is $1.04e^8$, and that of LS is $1.07e^9$.

Fig. 6 depicts the distribution of the SAMP-based reconstructed distinct energy clusters of the sparse channel representation $\widehat{\mathbf{H}}_b$ with different SNRs. The channel model is built as 4 clusters, each with 1 ray. The number of antennas of both sides is $N_t = N_r = 32$. The results presented in Fig. 6 validate that the dictionary matrices $\overline{\mathbf{A}}_t$ and $\overline{\mathbf{A}}_r$ indeed transform the channel to its sparse counterpart and can be leveraged for the subsequent estimation procedure. Specifically, for an $N_p = 4$ multipath physical channel, the corresponding $\widehat{\mathbf{H}}_b$ exhibits four distinct clusters with varying SNRs. As shown, when SNR=5 dB, the clusters are slightly decentralized with small fluctuations outside. However, thanks to the mitigation of noise interference, the clusters are sharpened with little channel energy distributed outside when SNR=25 dB. This figure shows that there are powerful multipaths of different directions in transmission space. These results can be leveraged to form a space division multiplexing transmission system and improve the efficiency of the communication, which will be discussed in our future work.

Fig. 7 shows the MSE performance of SAMP compared with LS along with different sparsity levels. The simulation is performed with SNR=5 dB, 15 dB and 25 dB. The number of antennas of both sides is $N_t = N_r = 32$. In the channel model, the number of clusters is varied, but each with only one ray. The parameter of gird size G is 64. As shown in Fig. 7, as the sparsity level increases, the performance of LS changes quite slightly, whereas the performance of SAMP exhibits a large difference. Specifically, we observe that when SNR=25 dB, the performance of a sparsity level of 50 is much worse than that of a sparsity level of 4 in the SAMP-based results, whereas the LS's results remain steady. This is because the LS algorithm is based on a matrix inversion method, whereas SAMP is a compressed sensing solution whose performance relies greatly on the sparsity level of the system. Moreover, we observe that along with increasing SNR, the performances of SAMP and LS are both much better, and this result is evidently due to the lower noise interference. Furthermore,

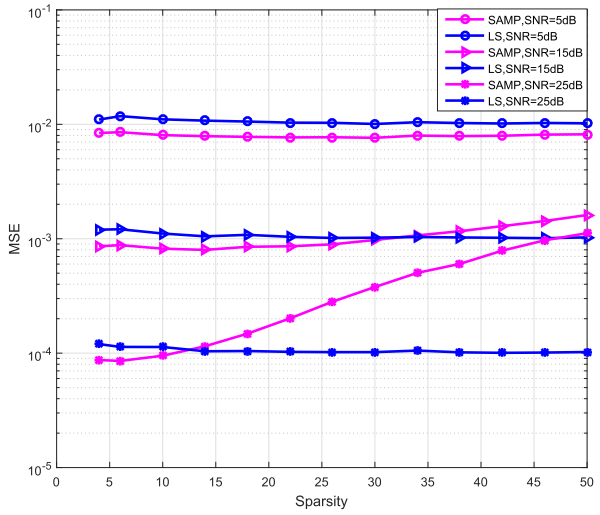

FIGURE 7. MSE performance of SAMP compared with LS along with different sparsity levels.

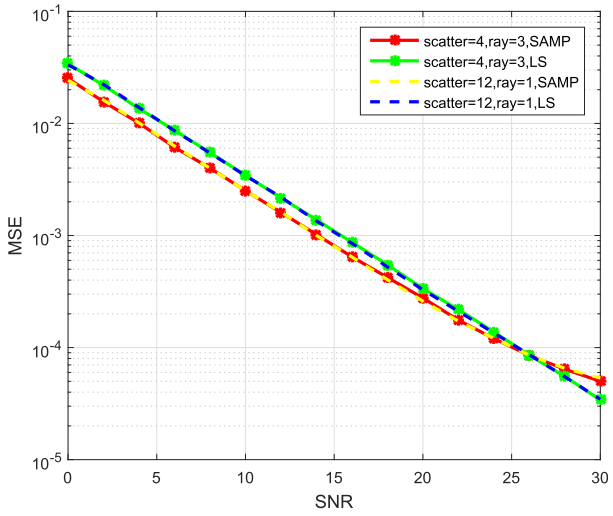

FIGURE 8. Comparison of the difference of two generation modes of multipaths in terms of MSE.

when comparing the results of SAMP with different SNRs, we observe that with high SNRs, the MSE performance is much different along with the sparsity level. This is because the sparsity parameter does not make a difference in the MSE when the SNR is low enough, which means that both the SNR and the sparsity level determine the system performance.

In Fig. 8, we compare the performance difference of two generation modes of multipaths. One channel model is that the number of clusters is 4, with 3 rays in each, and the other is with 12 clusters and 1 ray in each. Both models have the same sparsity level. The number of antennas of both sides is $N_t = N_r = 32$. The parameter of gird size G is 64. In the simulation, we observe that the performances of the two modes are almost identical whether based on the SAMP algorithm or the LS algorithm. The curves in the figure produced by SAMP and LS are nearly overlapped with each other. This

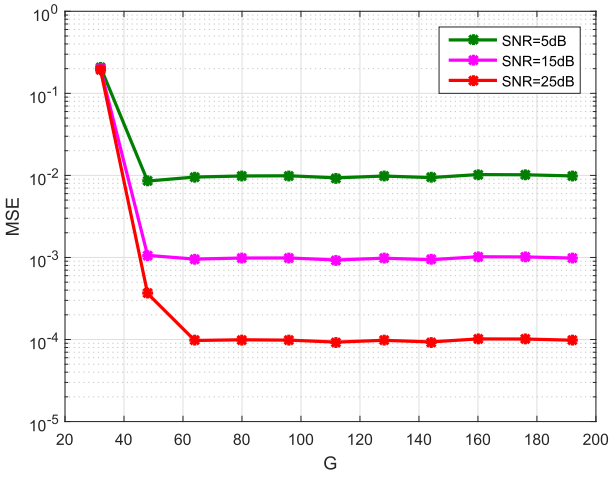

FIGURE 9. Influence of the grid size G on MSE performance in the SAMP algorithm.

result indicates that the two modes of multipath generation do not impact the system performance as long as they share the same sparsity level.

Fig. 9 presents the influence of the grid size G on MSE performance in the SAMP algorithm. The parameter of the number of antennas is $N_t = N_r = 32$. The channel model used is 4 clusters, each with 1 ray. The observation results are evaluated at SNR=5 dB, 15 dB and 25 dB. As shown in this figure, the MSE performances are first improving as the SNR increases. Moreover, for each curve in the figure, when G becomes larger, the MSE decreases. This result occurs because a larger G could mitigate angle error when estimating the channel. Note that for $N_t = N_r = 32$, the MSE performance stabilizes when G$\geq$64, and increasing G could not further reduce the estimation error. This result means that we do not need to choose an infinite G to obtain satisfactory results; rather, we can just choose the smallest G that begins to make the results stable. Additionally, this is the reason why we choose G=64 for the other simulations when the antenna number is $N_t = N_r = 32$.

VI. CONCLUSION

In this paper, based on phased array radar, we proposed a ray-cluster-based spatial channel model and a sounding channel estimation scheme for integrated radar and communication systems. The channel was modeled by physical multipaths between the transmitter and receiver, each with an attenuation and AOA/AOD. The number of beams needed to cover the space was analyzed in terms of resolvability in the angular domain. The directional beamforming vectors were presented to probe the channel. Redundant dictionary matrices were utilized to present the channel as a sparse signal recovery problem, and the SAMP-based algorithm was leveraged to solve this problem. The experimental results show that the proposed method could solve the channel estimation problem with reduced complexity and outperform the LS algorithm by 25% in general. Future work will focus on the space division

multiplexing transmission problem based on our channel estimation results of integrated radar and communication systems.

REFERENCES

[1] S. Quan, W. Qian, J. Guq, and V. Zhang, "Radar-communication integration: An overview," in *Proc. 7th IEEE Int. Conf. Adv. Infocomm Technol.*, Nov. 2015, pp. 98–103.

[2] Y. Zhang, L. Huang, and J. Song, "Phased array radar based angular domain channel estimation scheme for integrated radar-communication system," in *Proc. IEEE Military Commun. Conf. (MILCOM)*, Nov. 2016, pp. 906–911.

[3] X. Li, R. Yang, Z. Zhang, and W. Cheng, "Research of constructing method of complete complementary sequence in integrated radar and communication," in *Proc. IEEE 11th Int. Conf. Signal Process. (ICSP)*, vol. 3. Oct. 2012, pp. 1729–1732.

[4] L. Han and K. Wu, "Joint wireless communication and radar sensing systems—State of the art and future prospects," *IET Microw., Antennas Propag.*, vol. 7, no. 11, pp. 876–885, 2013.

[5] M. Braun, R. Tanbourgi, and F. K. Jondral, "Co-channel interference limitations of ofdm communication-radar networks," *EURASIP J. Wireless Commun. Netw.*, vol. 2013, no. 1, p. 207, Dec. 2013.

[6] A. Ouacha, A. Fredlund, J. Andersson, H. Hindsefelt, V. Rinaldi, and C. Scattoni, "SE-IT joint M-AESA program: Overview and status," in *Proc. IEEE Int. Symp. Phased Array Syst. Technol. (ARRAY)*, Oct. 2010, pp. 771–776.

[7] G. C. Tavik *et al.*, "The advanced multifunction RF concept," *IEEE Trans. Microw. Theory Techn.*, vol. 53, no. 3, pp. 1009–1020, Mar. 2005.

[8] J. P. Stralka and G. G. L. Meyer, "OFDM-based wideband phased array radar architecture," in *Proc. IEEE Radar Conf. (RADAR)*, May 2008, pp. 1–6.

[9] J. A. Molnar, I. Corretjer, and G. Tavik, "Integrated topside—Integration of narrowband and wideband array antennas for shipboard communications," in *Proc. IEEE Military Commun. Conf. (MILCOM)*, Nov. 2011, pp. 1802–1807.

[10] Z. Wu, Y. Zhang, and Z. Hang, "A burst SC-FDE scheme for high-speed communication based on radar," in *Proc. IEEE Military Commun. Conf. (MILCOM)*, Nov. 2013, pp. 1541–1546.

[11] L. Li, G. Li, and C. Li, "Communication system based on active phased array radar," *J. China Acad. Electron.*, vol. 3, no. 2, pp. 131–135, 2008.

[12] G. Zhang, *Principles of Phased Array Radar*. Beijing, China: National Defense Industry Press, 2010.

[13] E. Brookner, "Phased-array radars," *Sci. Amer.*, vol. 252, no. 2, pp. 94–102, 1985.

[14] J. Lee, G.-T. Gil, and Y. H. Lee, "Channel estimation via orthogonal matching pursuit for hybrid mimo systems in millimeter wave communications," *IEEE Trans. Commun.*, vol. 64, no. 6, pp. 2370–2386, Jun. 2016.

[15] D. Tse and P. Viswanath, *Fundamentals of Wireless Communication*. Cambridge, U.K.: Cambridge Univ. Press, 2005.

[16] J. Singh and S. Ramakrishna, "On the feasibility of codebook-based beamforming in millimeter wave systems with multiple antenna arrays," *IEEE Trans. Wireless Commun.*, vol. 14, no. 5, pp. 2670–2683, May 2015.

[17] A. S. Y. Poon, R. W. Brodersen, and D. N. C. Tse, "Degrees of freedom in multiple-antenna channels: A signal space approach," *IEEE Trans. Inf. Theory*, vol. 51, no. 2, pp. 523–536, Feb. 2005.

[18] M. Yang, L. Zhang, J. Yang, and D. Zhang, "Metaface learning for sparse representation based face recognition," in *Proc. 17th IEEE Int. Conf. Image Process. (ICIP)*, Sep. 2010, pp. 1601–1604.

[19] R. G. Baraniuk, "Compressive sensing [lecture notes]," *IEEE Signal Process. Mag.*, vol. 24, no. 4, pp. 118–121, Jul. 2007.

[20] T. T. Do, L. Gan, N. Nguyen, and T. D. Tran, "Sparsity adaptive matching pursuit algorithm for practical compressed sensing," in *Proc. 42nd Asilomar Conf. Signals, Syst. Comput.*, Oct. 2008, pp. 581–587.

[21] S. F. Cotter and B. D. Rao, "The adaptive matching pursuit algorithm for estimation and equalization of sparse time-varying channels," in *Proc. Conf. Rec. 34th Asilomar Conf. Signals, Syst. Comput.*, vol. 2. Oct. 2000, pp. 1772–1776.

LING HUANG received the B.E. degree from Beihang University, Beijing, China, in 2013. She is currently pursuing the Ph.D. degree at Tsinghua University, Beijing. Her research interests include communication systems and signal processing.

YU ZHANG (M'07–SM'12) received the B.E. and M.S. degrees in electronics engineering from Tsinghua University, Beijing, China, in 1999 and 2002, respectively, and the Ph.D. degree in electrical and computer engineering from Oregon State University, Corvallis, OR, USA, in 2006.

In 2007, he was an Assistant Professor with the Research Institute of Information Technology, Tsinghua University, for eight months. He is currently an Associate Professor with the Department of Electronic Engineering, Tsinghua University. His current research interests include the performance analysis and detection schemes for MIMO-OFDM systems over doubly selective fading channels, transmitter and receiver diversity techniques, and channel estimation and equalization algorithm.

QINGYU LI received the B.E. degree from Tsinghua University, Beijing, China, in 2014, where she is currently pursuing the Ph.D. degree. Her research interests include communication systems, information theory, and signal processing.

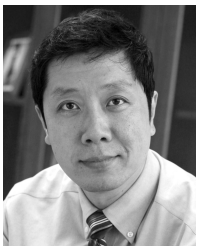

JIAN SONG (SM'10–F'16) received the B.Eng. and Ph.D. degrees from the Electronic Engineering Department, Tsinghua University, Beijing, China, in 1990 and 1995, respectively. He was with Tsinghua University upon his graduation. He then conducted post-doctoral research work with The Chinese University of Hong Kong and the University of Waterloo, Canada, in 1996 and 1997, respectively. He joined the industry in 1998 and was with the Advance Development Group, Hughes Network Systems, USA, for seven years before joining the faculty team in Tsinghua as a Full Professor in 2005. He is currently the Director of the DTV Technology R&D Center, Tsinghua University, and the Director of the Key Laboratory of Digital TV System, Shenzhen, China.

His current research interests include digital broadcasting, wireless communications, powerline communications, and visible line communications. He has authored over 240 peer-reviewed journal and conference papers, and holds two U.S. and over 50 Chinese patents with several pending. He is a co-author of three books in DTV area and a co-translator of one book in PLC area.

Dr. Song is an IET Fellow. He is an AdCom member of the IEEE Broadcasting Technology Society. He is very active in serving the IEEE community. He founded the IEEE BTS Beijing Chapter in 2007 and has been the Chairman since then. He has served as the technical committee members, panelists for many conferences, and also given invited talks. He has successfully organized several IEEE conferences, such as the IEEE BMSB 2014, the IEEE Healthcom 2012, and the IEEE ISPLC, as the general or TPC chair. He serves as an Associate Editor of the IEEE TRANSACTIONS ON BROADCASTING.